ISSN 0023-1584, Kinetics and Catalysis, 2006, Vol. 47, No. 4, pp. 469–480. © MAIK "Nauka/Interperiodica" (Russia), 2006.
Original Russian Text © E.A. Cherezov, E.V. Kovalev, V.I. Elokhin, A.V. Myshlyavtsev, 2006, published in Kinetika i Kataliz, 2006, Vol. 47, No. 4, pp. 485–497.

Statistical Lattice Model for the Bimolecular Reaction on the Dynamically Changing Surface of a Body-Centered Metal Crystal

E. A. Cherezov[a,b], E. V. Kovalev[b], V. I. Elokhin[b], and A. V. Myshlyavtsev[c,d]

[a] *Tuvinian Institute for the Exploration of Natural Resources Development, Siberian Division, Russian Academy of Sciences, Kyzyl, 667007 Tuva Republic, Russia*

[b] *Boreskov Institute of Catalysis, Siberian Division, Russian Academy of Sciences, Novosibirsk, 630090 Russia*

[c] *Institute of Hydrocarbons Processing, Siberian Division, Russian Academy of Sciences, Omsk, 644040 Russia*

[d] *Omsk State Technical University, Omsk, 644050 Russia*

e-mail: elokhin@catalysis.ru

Received April 7, 2004

Abstract—A statistical lattice model has been constructed for the surface of a body-centered cubic (bcc) crystal whose morphology varies under the action of external factors (temperature and adsorbate coverage). Monomolecular and dissociative bimolecular adsorption on the bcc crystal surface has been investigated. In this model, adsorption smoothens the originally rough surface owing to adsorbate molecules stabilizing their flat adsorption areas, as distinct from adsorption on the primitive cubic lattice. Our model differs from the models with invariable surface morphology in that the number of its accessible adsorption sites is variable and depends on external conditions. The kinetics of a catalytic reaction proceeding by the Langmuir–Hinshelwood mechanism have been studied for the (100) face of a bcc crystal whose morphology varies under the action of the reaction medium.

DOI: 10.1134/S002315840604001X

The hypothesis that an adsorbed layer is ideal is the simplest assumption made in the description of adsorption and reactions on the solid surface, although it has long been known that this hypothesis is not true even for metal single crystals. Obviously, physically substantiated mathematical models of processes on catalytic surfaces [1, 2] are required for correct interpretation of experimental data. Such models must somehow take into account the nonideality of the adsorbed layer. This problem is solved in part by using analytical models constructed in the framework of Roginskii's classification of nonidealities (inherent and induced inhomogeneities of the adsorbed layer), e.g., Temkin's logarithmic isotherm for the uniformly inhomogeneous surface. However, in these models, it is difficult to take into account the simultaneous effect of factors associated with inherent and induced inhomogeneities on the kinetics of reactions occurring on real catalytic surfaces. Moreover, within a deterministic (analytical) model, it is very difficult to take into account the dynamic morphological changes (roughening) of the surface during the reaction, which take place in real systems owing to the thermal diffusion of surface metal atoms or to the phase transitions accompanying the adsorption-induced reconstruction of the surface. It was demonstrated experimentally that the surface structure is not invariable and can undergo substantial morphological changes in the course of a heterogeneous catalytic reaction. Moreover, these changes can determine the dynamics of the process as a whole [3–7]. This adjustment of the surface to the reaction confirms Boreskov's statement that the environment influences the catalyst. As follows from experimental data, various reaction- and/or heat-induced surface defects (terraces, steps, kinks, adatoms, and vacancies) exert marked effects on catalytic reactions.

Therefore, it is important to construct theoretical models allowing for reaction-induced dynamical morphological changes of the surface. The most efficient approach to the simulation of the spatiotemporal dynamics of adsorbed substances on real catalytic surfaces, whose structure and properties may vary under the action of the reaction, is the construction of Monte Carlo stochastic models [8]. In the Monte Carlo method, the dynamics of processes on the catalytic surface is treated as a Markovian chain of elementary events (adsorption, reaction, diffusion, local surface reconstruction, etc.) occurring at the active sites of the catalyst. The aforementioned sites are imitated by the cells of a lattice with a preset rigid or a dynamically changing (flexible) structure. An obvious drawback of stochastic models is that they require large amounts of

calculation. The main advantages of these models that are most significant for solving the above problem are as follows: (1) it is possible to independently consider the local environment of each adsorbed molecule or each active or inactive site on the surface; (2) any idea of the surface process allows rather easy algorithmic realization in terms of the generalized model of lattice gas; (3) various physicochemical processes with the rate coefficients determined either experimentally or by molecular dynamics methods (including processes that cannot be described using analytical models), can be included in the model; (4) the surface being modeled can be immediately visualized. Taking into account the spatiotemporal changes of the surface on the atomic–molecular level provides a deeper insight into the mechanisms of heterogeneous catalytic reactions and markedly facilitates the interpretation of physicochemical data.

Imitation (or stochastic) simulation based on the Monte Carlo method is an efficient and general-purpose way of describing the dynamic spatiotemporal behavior of adsorbates on a real catalytic surface whose structure varies under the action of external factors. At present, imitative simulation is widely used in theoretical studies of various processes on solid surfaces. Solid-state physicists extensively investigate models that take into account the dynamic behavior of the metal surface exposed to external factors, such as temperature (models of crystal growth, surface reconstruction, etc.) [9, 10]. In recent years, stochastic models have been suggested for adsorption and reactions on surfaces with a dynamically changing morphology. Most of these models can be divided into two groups according to the method of construction and underlying physical principles.

The first group is made up of models describing structural phase transitions (SPTs) of metal surfaces reconstructed so that the surface atomic layer differs in symmetry from the face bulk. The surface layer of {100} and {110} single crystals of transition metals (e.g., Pt, Ir, Cu, W, Au, and Ag) undergoes an SPT (surface reconstruction) under the action of adsorbed substances such as CO, NO, H_2, and C_2H_4. Adsorption causes a local decrease in the free energy of the surface, resulting in the restoration of the bulk atomic periodicity in the surface atomic layer (lifting of reconstruction). This is usually accompanied by dramatic changes in the adsorption properties of the metal. For example, the sticking coefficient of oxygen on the Pt(100)-(1×1) surface, which results from CO adsorption, is approximately two orders of magnitude larger than the same coefficient for the bare initial Pt(100)-hex surface. The adsorption of NO, H_2, and CO molecules on the Pt(110) also lifts the surface reconstruction, leading to a $(1 \times 1) \longrightarrow (1 \times 2)$ transition and to a 2- to 3-fold increase in the O_2 sticking coefficient. Furthermore, if the adsorbate–substrate (metal) binding energy is comparable to or exceeds the interatomic bond energy in the metal, there can be changes in the metal surface morphology. Among the earlier theoretical studies of the dynamic behavior of simple molecules on reconstructive surfaces, note the studies dealing with the systems H/W(001) [11], CO/Pt(110) [12], H/Cu(110) [13], and O/Ag(110) [13].

Apparently, the first successful attempt to simulate the surface SPT $(1 \times 1) \rightleftharpoons (1 \times 2)$ on the Pt(110) face involved in CO oxidation by the Langmuir–Hinshelwood (LH) mechanism was made by Imbihl et al. [14]. The driving force of this transition is the CO adsorption–induced transfer of part of the surface platinum atoms, which causes the formation or disappearance of the (1×2) added/missing row structure. The SPT simulation algorithm consisted of two repeating steps, namely, the calculation of reaction kinetics (CO adsorption and desorption, O_2 adsorption, and CO_2 formation) and surface reconstruction according to the local CO_{ads} distribution. The second step leads to surface roughening. A long-term numerical experiment shows the formation of a sawtooth faceted surface structure. It was also demonstrated [14] that the deep (1×2) added/missing row structure appears in the model only if the surface steps and terraces differ rather widely in terms of the oxygen sticking coefficient for active sites. This model is consistent with a wide variety of experimental data, including those for surface smoothening (the reverse transition $(1 \times 2) \longrightarrow (1 \times 1)$) after the termination of the reaction (removal of the gas phase).

The surface transition (hex) $\rightleftharpoons$ (1×1) on the Pt(100) face proceeds in another way. The thermodynamically stable (clean) Pt(100) surface has an hcp structure, in distinction to the square symmetry of the face bulk. The adsorption of CO or NO leads to the lifting of reconstruction yielding the Pt(100)-(1×1) surface, whose atomic density is ~20% lower than the atomic density of the reconstructed surface Pt(100)-(hex). The excess Pt atoms resulting from this SPT are "squeezed" onto the Pt(100)-(1×1) surface, forming, through migration, Pt(100) islands with the same (1×1) structure. This process was simulated by Reynolds et al. [15], who studied the mean size of Pt(100) islands "squeezed" onto the surface layer as a function of the temperature and energy parameters of the surface, specifically, the metal–metal atomic attraction energy *V*. Adsorption and surface reaction were taken into account indirectly. It was assumed that CO adsorption induces a phase transition and, as time passes, new platinum atoms (up to 20% of the full surface coverage) are forced onto the surface. It was found that qualitative agreement between the calculated and experimental data is achieved at intermediate, not high or low, *V* values of ~20 kJ/mol, which coincides with the value measured by means of field ion microscopy (15–25 kJ/mol) [15]. At low *V* values, no large islands form because of thermodynamic limitations: low metal–metal bond energies are insufficient to prevent such islands from disintegration. At high *V* values, the

rapidly forming small two-dimensional islands are "excessively" stable and do not grow because of kinetic limitations.

Monine and Pismen [16–18] suggested an original stochastic model for SPT associated with the oscillatory dynamic of CO oxidation on the Pt(110) surface. The oscillatory variation of the CO coverage of the surface was simulated using the Ginzburg–Landau phenomenological equation. The Pt(110) surface was viewed as a face-centered cubic lattice with lateral interactions between nearest-neighbor sites, which were assumed to be capable of migrating on the surface, obeying specified rules. In particular, it was assumed that only atoms whose nearest neighbors are not atoms from an upper layer can move. The Metropolis algorithm (see below) was used to deduce the equilibrium surface morphology under given conditions. Numerical experiments have demonstrated that a variety of scenarios are possible for the morphological changes of the surface induced by repeating $(1 \times 1) \rightleftharpoons (1 \times 2)$ reconstruction cycles accompanying the kinetic self-oscillations. In turn, the steadily growing surface roughness alters the kinetic parameters of the reaction so as to lengthen the mean oscillation period.

The second group of models includes stochastic models for physicochemical processes on the surface of an infinite Kossel crystal. The Kossel crystal model, which is well known in solid-state physics, is a very convenient object for investigating the thermal roughening of the surface of some metals: at low temperatures, the metal surface remains smooth and has a negligible number of point defects; at high temperatures below the melting point, thermal excitation can bring about persistent surface defects of various kinds (rough surface) [19–23]. This surface roughening is interesting both from the standpoint of the fundamental theory of surface phase transitions and from the practical standpoint, since many heterogeneous catalytic reactions proceed more rapidly on rough surfaces and on well-faceted, supported nanoparticles. The Kossel crystal [24] is a two-dimensional set of columns, whose upper elements (atoms) can move (diffuse) to the vertices of neighboring columns, obeying the rules defined primarily by the lattice symmetry (see below). The modified Kossel crystal in which the overhang of atoms and vacancy formation in the bulk are forbidden is called the solid-on-solid (SOS) model. This model gave birth to the so-called terrace–step–kink (TSK) model of the solid surface.

Based on these concepts, we suggested a model for adsorption and reaction on a rough and flexible surface whose morphology depends on temperature and on the composition of the adsorbed layer [25–27]. It was demonstrated that, if the adsorbate interacts energetically with substrate atoms, adsorption isotherms for surfaces with dynamically changing morphology will have peculiarities differentiating then from adsorption isotherms for a rigid surface. In turn, surface morphology is markedly affected by the adsorbed layer. We considered the catalytically active metal surface as a Kossel crystal or, more precisely, as an SOS model for a crystal with a primitive cubic structure [20].

Using the restricted solid-on-solid (RSOS) model, a modification of the SOS model in which the difference between the heights of nearest-neighbor columns cannot exceed unity, Zhdanov and Kasemo [28, 29] demonstrated that adsorption and reaction in an adsorbed layer admitting adsorbate–metal surface interaction can markedly reduce the surface roughening temperature T_R. This effect is due to the additive influence of three types of lateral interactions: (1) nearest-neighbor (nn) adsorbate–substrate attraction, (2) next-nearest-neighbor (nnn) adsorbate–substrate repulsion, and (3) nearest-neighbor (nn) adsorbate–adsorbate repulsion. The energies of these interactions are of the same order of magnitude as the substrate–substrate interaction energy and fall in the range from 4 to 10 kJ/mol. Furthermore, we found [25–27] that the surface roughness, which can be defined as the mean difference between column heights in the SOS model, will greatly increase if the interaction between neighboring metal and adsorbate atoms is taken into account. However, we did not perform any detailed study of the effect of the lateral interactions on the surface roughening temperature. The adsorbate-induced roughening of the surface can exert a very strong effect on the catalytic reaction even at a low roughness [29]. If this is the case, the reaction kinetics can change both quantitatively and qualitatively. It was also demonstrated that the roughening dynamics of an initially smooth surface (at $T > T_R$) and the dynamics of the reverse relaxation of the preliminarily roughened surface (at $T < T_R$) are logarithmic functions of time t [28, 29]. In particular, the mean-square difference between column heights at $T > T_R$ in the RSOS model grows with time as $\ln t$. Another roughening mechanism was suggested in a later publication [30]. That mechanism can take place during an exothermic reaction on a metal or oxide catalyst when the energy released in adsorption or reaction events is transferred to the surface atoms of the catalyst. Two fundamentally different regimes can be distinguished here: (1) $T > T_R$, when the thermodynamically possible phase transition is suppressed by kinetic limitations, but the energy resulting from the exothermic reaction nevertheless favors surface roughening; (2) $T < T_R$, when the thermal smoothening of the surface takes place, but this process competes with surface roughening due to exothermic adsorption events and to the interaction between adsorbates yielding reaction products. It is also possible that both mechanisms act simultaneously to increase surface roughness. This is particularly likely when the catalytic reaction proceeds at a high specific rate.

One of the few studies devoted to the stochastic simulation of the above phenomena in particular systems is a study by Aldao et al. [31], who attempted to construct

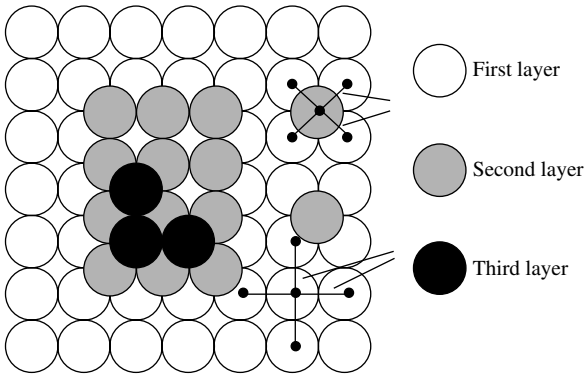

Fig. 1. Hard-sphere representation of the BCSOS model.

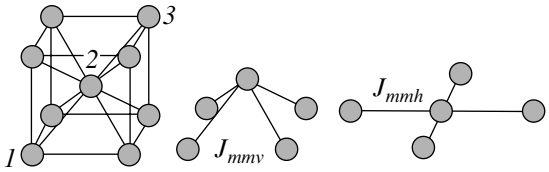

Fig. 2. Unit cell of the bcc lattice. (*1–3*) The numbers of layers shown in Fig. 1.

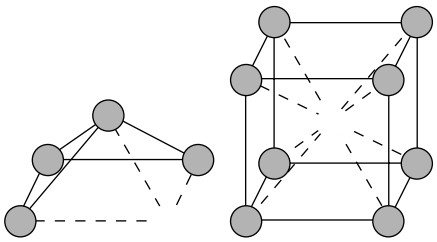

Fig. 3. Forbidden states in the BCSOS model.

a Monte Carlo model (based on the concept of a cubic Kossel crystal) for the experimentally observed phenomenon of the roughening of the Si(100) surface upon low-temperature chlorine adsorption. In this model, it is assumed that the driving force of surface roughening is the lateral repulsion between adsorbates, which weakens the substrate–substrate bonding. It was demonstrated that this model accounts satisfactorily for the STM mean sizes of the valleys and islands resulting from chlorine adsorption on Si(100) only at medium Cl coverages [31]. The authors of this model believe that a better fit to experimental data can be achieved by taking into account the effects arising from the anisotropy of the Si(100) surface and other adsorbate–substrate lateral interactions [28, 29] causing surface roughening.

Finally, note studies by Vakarin et al. [32, 33], who considered the effect of the adsorbed layer on the substrate in the case of interfacial liquid–solid interaction. Using generalized lattice gas theory and numerical simulation by Brownian dynamics methods, it was demonstrated that competing displacing interactions in the adsorbed layer can cause distortions in the underlying substrate.

In most of the above-mentioned works, the structure of the catalyst (metal) was viewed, for the sake of simplicity, as a primitive cubic lattice. However, only a few metals have a primitive cubic structure (e.g., K and Na). Most metals employed in catalysis have a bcc, fcc, or hcp structure. This study is devoted to the stochastic simulation of adsorption and reaction on the rough surface of an infinite bcc crystal whose morphology varies under the action of external factors (temperature and adsorbate coverage). The purpose of this study is to gain insight into the reciprocal effects of the reaction kinetics and equilibrium surface morphology at varying system parameters (temperature, the partial pressures of the reactants, lateral interactions between adsorbed atoms and metal atoms, etc.) and into the effect of the crystal structure on the reaction kinetics (primitive cubic and bcc lattices will be compared). Simulation will be carried out for a reaction that proceeds by a standard LH mechanism and qualitatively reflects many specific features of the oxidation of simple molecules on platinum-group metals.

MODELS AND ALGORITHMS

Model of the Crystal Surface

The dynamically changing catalyst surface was described in terms of the Kossel crystal model, whose particular case is the SOS model. This model is well known in solid-state physics and is capable of predicting a roughening transition for some metals. Earlier [25–27], the simulation of dynamically changing surface morphology was carried out for a crystal with a primitive cubic lattice. Here, we consider a bcc lattice [20–22] based on a square two-dimensional lattice of dimensions $N \times N$ subject to periodical boundary conditions. This model, called the body-centered-solid-on-solid (BCSOS) model, was suggested by van Beijeren [19]. It can be represented as a set of solid spheres (Fig. 1). In each layer of the crystal, the centers of the spheres are at square lattice sites (Fig. 2), each sphere being in contact with four other spheres located in the underlying layer—the contact condition. A layer can be incomplete, but this condition must always be met. Thus, this model forbids overhanging atoms and vacancies in the substrate bulk (Fig. 3). These conditions limit the applicability of the model to a temperature range that is not close to the melting point of the crystal. The columns of the spheres are divided into two subsets. Under the assumption that the distance between two nearest-neighbor spheres in one column is equal to unity, two nearest-neighbor columns belonging to different subsets differ in height by either +1/2 or –1/2 and two nearest-neighbor columns belonging to the same subset differ in height by +1, 0, or –1.

The surface morphology changes owing to the thermal diffusion of surface metal atoms. Metal atoms in the crystal lattice attract one another. The simplest variants of their interaction are displayed in Figs. 1 and 2, where J_{mmh} is the energy of interaction between nearest-neighbor atoms in one layer and J_{mmv} is the energy of interaction between an atom in a given layer with atoms of the underlying layer under the above contact condition. The diagonal interactions between atoms on one level and the interactions with farther atoms are neglected for the sake of simplicity and clarity. In the calculation of the probability of a surface atom passing from one place to another as a result of diffusion, the interaction characterized by the energies J_{mmv} can also be neglected: in the case of an infinite crystal (periodic boundary conditions) obeying the contact condition, the contribution from these interactions to the total crystal energy is invariable. The ground state of the system at low temperatures is the state in which each metal atom has the largest number of lateral neighbors. In this case, the surface has the smallest number of defects and has a bcc(100) structure. As the temperature is raised, the surface morphology begins to change. This phenomenon was simulated using the Metropolis algorithm [34] realized as follows:

(1) Randomly choose a surface atom and a surface site possible for its new location. The new location of the atom may be separated by any distance from the initial location (this is so-called mathematical diffusion, in which any transfer is instantaneous and, irrespective of the distance).

(2) Verify that the atom can occupy the new site (the contact condition is satisfied). If the transfer is allowable, then it is characterized by some probability, which is estimated as follows. If the energy of the system is decreased as a result of this transfer (that is, the number of nearest neighbors is increased) or is not changed, than this event takes place with a probability equal to unity. If the energy of the system decreases, then the probability of transfer is

$$W = \exp\left(\frac{-\Delta E}{kT}\right) < 1,$$

where ΔE is the difference between the final and initial energies of the system, T is the temperature, and k is the Boltzmann constant. The energies of the initial and final (possible) states are calculated as $E_i = \Sigma J_{mmh}$ (additive interactions).

This algorithm ensures that the Boltzmann distribution is fulfilled for the probabilities of possible system configurations and that the thermodynamic equilibrium is reached in an infinite number of Monte Carlo steps (in our case, one Monte Carlo step consists of N^2 trials of diffusion transfer of surface atoms of the crystal). In real calculations, a rather large, but not infinite, number of steps are made, after which the configuration of the system can be considered to be equilibrated (within the range of statistical fluctuations). Usually, we made ~50000 Monte Carlo steps, since further increasing their number did not cause any visible changes in the surface morphology.

Obviously, the determining parameter in our model is the metal–metal interaction energy J_{mmh}. Unfortunately, there are no reliable experimental or theoretical data for this parameter; for this reason, we will not deal with particular supports, metals or adsorbates. A rough estimate of this quantity is provided by the formation energy of an adatom–vacancy pair on a smooth (100) surface calculated in the framework of effective medium theory (see [22] and references therein). This energy is ~0.115 eV [22] or ~10 kJ/mol. Here, based on data reported in [25–27], we set J_{mmh} = –4 kJ/mol (attraction). Varying this energy changes the roughness transition temperature: the stronger the interatomic interaction, the higher the calculated equilibrium temperature for a given surface relief.

Reaction Model and Kinetic Simulation Algorithm

Here, we model steady-state kinetic relationships for a catalytic reaction whose detailed mechanism includes the following elementary steps:

$$1.\ Z + A \longrightarrow AZ,$$
$$1'.\ AZ \longrightarrow Z + A,$$
$$2.\ 2Z + B_2 \longrightarrow 2BZ,$$
$$3.\ AZ + BZ \longrightarrow 2Z + AB,$$

where Z is an active site on the catalyst surface. This is the LH mechanism, which is valid for many chemical reactions, including CO oxidation on platinum metals (A = CO and $B_2 = O_2$).

The reaction rate and intermediate-product coverage data calculated here as a function of gas pressure will be compared with the same data presented in a seminal publication by Ziff et al. [35]. That publication, which has very frequently been quoted in the last decade, presents one of the earliest attempts at the statistical lattice simulation of catalytic reactions. In that work, the kinetics of a reaction consisting of elementary steps 1, 2, and 3 were investigated by the kinetic Monte Carlo (kMC) method under the oversimplifying assumptions that there is no desorption or surface diffusion of adsorbates at an infinitely high reaction rate. This stochastic model revealed a variety of interesting facts, including the finiteness of the range in which the reaction rate is nonzero, the occurrence of two kinetic phase transitions (a first-order transition, in which surface coverages change stepwise, and a second-order transition, in which the surface coverages change continuously, but their derivatives show a discontinuity), and adsorbate clustering. This model was given the

name of Ziff–Gulari–Barshad (ZGB) and triggered off more than a hundred of publications (for a review, see [36, 37]). In those publications, the model was complicated and its dynamic behavior was studied in greater detail (adsorbate diffusion and desorption, the finiteness of the reaction rate, lateral adsorbate–adsorbate interactions, different lattice types, etc., were taken into consideration). As far as we know, we are the first to apply the ZGB model to a bcc crystal.

Our reaction model takes into account the following processes: the monomolecular adsorption of the substance A, the bimolecular dissociative adsorption of the substance B_2, the desorption of A, the reaction between the adsorbed substances AZ and BZ, and the "mathematical" diffusion of metal atoms and AZ. The diffusion of BZ is neglected in the reaction model; however, this process is taken into account in the simulation of bimolecular adsorption isotherms (see below).

Let us discuss, in brief, the assumptions that we make in the simulation of the effect of dynamically inhomogeneous surface morphology on the kinetics of the model reaction $A + B_2$ proceeding by the LH mechanism. We assume that adsorbed BZ species do not diffuse and no desorption according to the equation $2BZ \longrightarrow B_2 + 2Z$ takes place. Thermally induced morphological changes of real metal surfaces usually set in at temperatures of about 500 K. It is to these temperatures that our study refers. However, the degree of roughening of the crystal surface in our model depends on two parameters, namely, temperature, and the metal–metal-interaction energy J_{mmh}, whose precise value is unknown. These parameters are interrelated is some sense: the stronger the attraction between nearest-neighbor metal atoms, the higher the temperature at which significant changes in surface morphology occur. Furthermore, in the kMC simulation of some reactions (e.g., CO oxidation on platinum-group metals), it is generally assumed that the dissociatively adsorbed compound B_2 (oxygen) is not desorbed at the reaction temperature (400–500 K) and the rate of BZ (O_{ads}) diffusion on the surface at this temperature is negligible as compared to the AZ (CO_{ads}) diffusion rate. The first assumption is substantiated by the fact that the heat of adsorption of oxygen on various faces of platinum-group metals is ~80 kJ/mol higher than the heat of adsorption of CO [38]. The activation energies of diffusion of oxygen and CO differ by a similar value of 40–70 kJ/mol [39–42]. The activation energy of diffusion itself depends on the face of the metal and on adsorbate coverage; however, the general feature is that, at the temperatures considered, the oxygen diffusion rate coefficient is several orders of magnitude lower than the CO diffusion rate coefficient, substantiating the second assumption.

The chemical reaction is simulated using the following algorithm:

(1) Imitate the metal surface with an $N \times N$ square lattice subject to periodic boundary conditions and randomly choose a cell in this lattice.

(2) Generate a random number x in the interval [0, 1] and choose one of the elementary processes. Calculate the probabilities of elementary processes, w_i, using the following formulas:

$$w_{\text{ads, A}} = \frac{p_A}{p_A + p_{B_2} + k_{\text{des, A}}\exp(-E_{\min}/kT)},$$

$$w_{\text{des, A}} = \frac{k_{\text{des, A}}\exp(-E/kT)}{p_A + p_{B_2} + k_{\text{des, A}}\exp(-E_{\min}/kT)},$$

$$w_{\text{ads, B}_2} = \frac{p_{B_2}}{p_A + p_{B_2} + k_{\text{des, A}}\exp(-E_{\min}/kT)},$$

where p_i is the partial pressure of the ith adsorbate in the gas phase, $k_{\text{des,A}}$ is the desorption constant of AZ (if desorption is taken into account, then $k_{\text{des,A}} = 1$; otherwise, $k_{\text{des,A}} = 0$), $E_{\min}$ is the energy of the interaction between an adsorbed molecule of the compound A and the environment that minimizes this energy (for the attractive and repulsive interactions between AZ and the nearest-neighbor metal atoms, this environment should include the maximum and the minimum possible number of neighbors, respectively), and E is the energy of the interaction between AZ and the given environment. Note that the sum of the probabilities of all elementary processes can be below unity (if AZ desorption is taken into account). If this is the case, an empty process can take place, after which pass to step 5.

(3) Check the possibility of the chosen process taking place (the formation of a near-surface adsorbate layer is forbidden). If the chosen process is impossible in the chosen cell, pass to step 5. Depending on the process chosen, checking is carried out by one of the following procedures.

Adsorption of A. If the cell is occupied by adsorbate, then the adsorption event is ruled out. If the cell is empty and meets the geometric constraints, then adsorption takes place with a probability equal to 1. The geometrical constraints are determined by the crystal lattice type. In the case of the bcc lattice, as distinct from the primitive cubic lattice, not only an empty cell but also an even area is required for adsorbate accommodation (there must be precisely four atoms arranged in a square below, making possible the adsorption of A onto a four-coordinate site, in accordance with the contact condition).

Desorption of A. If the cell is empty or is occupied by adsorbed BZ, then the desorption event is ruled out. If the cell is occupied by adsorbed AZ, then the probability of desorption is 1. Note that the dependence of the AZ desorption probability on the metal environment of

the AZ species are taken into account in step 2 (if the adsorbate–metal interaction energy J_{ma} is specified).

Adsorption of B_2. If the cell is occupied by adsorbate or does not meet the geometrical constraints, then desorption is ruled out. Otherwise, the state of a randomly chosen nearest-neighbor cell is examined. If this cell is empty, meets the geometrical constraints, and lies on the same level as the previous cell (that is, two neighboring four-coordinate adsorption sites lying on one level are required), then the probability of B_2 adsorption is 1. Otherwise, adsorption is ruled out.

(4) Examine the environment of the adsorbed species (it is assumed that the reaction AZ + BZ proceeds at an infinite rate; that is, once adsorbed AZ and BZ atoms appear in adjacent cells on one level as a result of adsorption or diffusion trials, they are removed as a reaction product). The reaction takes place as soon as it can. The surroundings of the adsorbed species (AZ or BZ) is searched for reaction partners in a random way by examining all nearest-neighbor cells.

(5) Carry out M diffusion events involving metal and AZ atoms on the catalyst surface, as is described above, in order to arrive at an equilibrium configuration. In the case of AZ diffusion, fulfill step 4 after each diffusion event. After all of the M diffusion events are completed, pass to step 1.

The time unit was a Monte Carlo step consisting of $N \times N$ trials of choice and realization of basic elementary steps proceeding at a finite rate (steps 1, 1', and 2). On the average, each lattice cell is examined once in one step. The number of diffusion events (M) per process choice trial was usually 10 to 30.

In each step, we calculate the reaction rate as the number of AB pairs removed from the surface, as well as the adsorbate coverage of the catalyst surface. The adsorbate coverage was calculated as the ratio of the number of cells occupied by adsorbate to the total number of cells on the surface. Unlike the primitive cubic lattice, the bcc lattice allows two ways of defining the total number of cells. This number can be defined either as the number of cells accessible to the adsorbate or as the total number of cells, irrespective of their accessibility. In the former case, the total number of cells is variable and decreases with increasing roughness (this is a fundamental distinction between the bcc and primitive cubic lattices).

Adsorption Model

The above algorithm was used in the simulation of the reaction consisting of steps 1, 1', 2, and 3. Similar algorithms were employed in the simulation of isotherms of monomolecular and bimolecular dissociative adsorption on a surface with a dynamically changing morphology. In the case of monomolecular adsorption the desorption of the adsorbed atom AZ was taken into account, the adsorption of B_2 was ruled out, and step 4 of the algorithm was skipped. Likewise, in the case of dissociative bimolecular adsorption, we took into account the associative desorption of two BZ atoms. For this process to occur, it is necessary that the nearest-neighbor surface sites, randomly chosen on one level, contain BZ atoms. The probability of desorption was calculated using the formula

$$w_{\mathrm{des,\,B_2}} = \frac{k_{\mathrm{des,\,B_2}} \exp(-E/kT)}{p_{\mathrm{B_2}} + k_{\mathrm{des,\,B_2}} \exp(-E_{\min}/kT)}.$$

After each adsorption or desorption trial, we carried out an internal diffusion cycle involving AZ or BZ atoms and surface atoms of the metal.

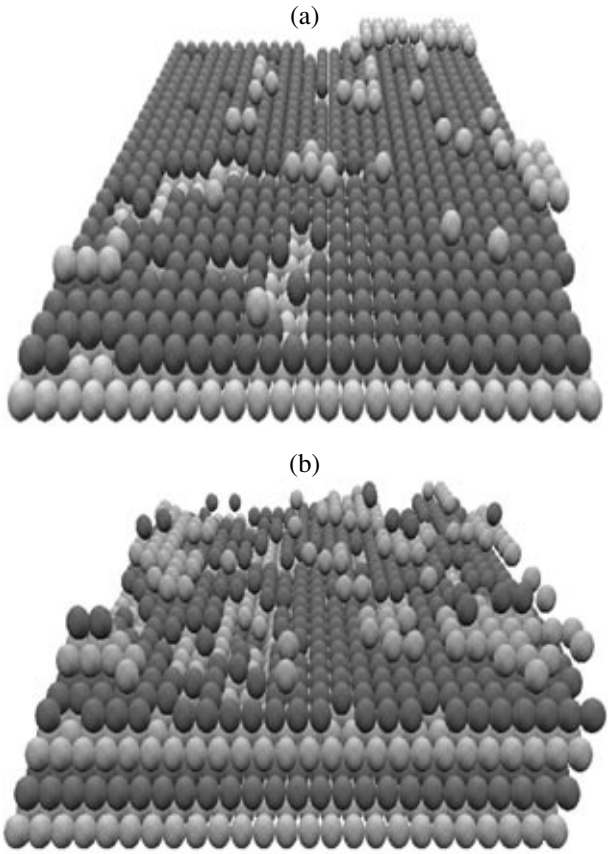

Fig. 4. Fragment of the surface at (a) 300 and (b) 1300 K.

RESULTS AND DISCUSSION

Modeling of the Rough Surface

The first step in our simulation procedure is the modeling of the equilibrium morphology of the crystal surface varying because of the diffusion of metal atoms in the absence of adsorbate. Some equilibrium surface morphology is established at each temperature. At low temperatures, the surface is almost smooth (Fig. 4a); as the temperature is raised, thermal excitation makes the surface rougher (Fig. 4b): the number of point defects

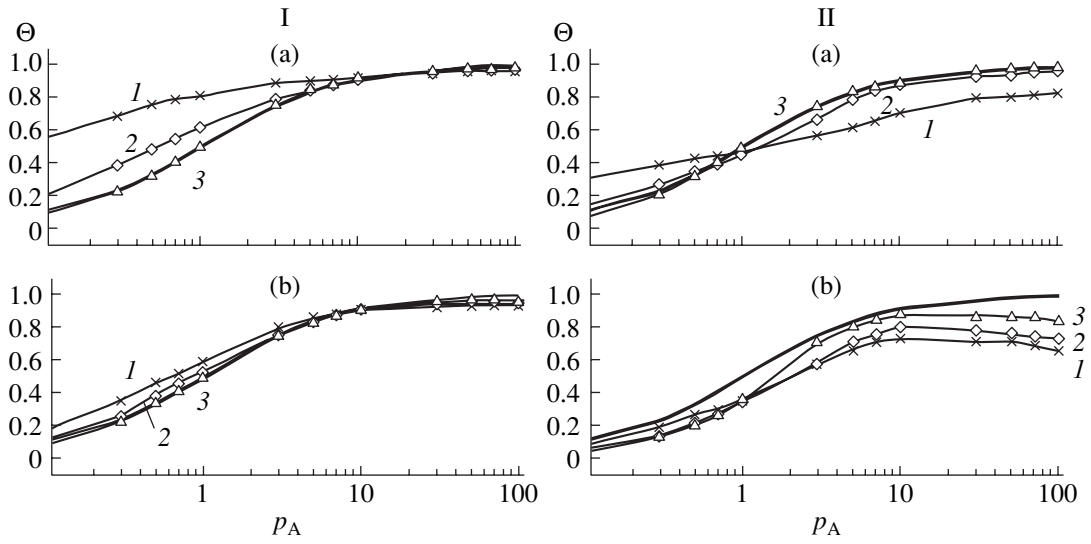

Fig. 5. Monomolecular adsorption isotherms at (Ia, IIa) 300 and (Ib, IIb) 1300 K: (*1*) $J_{ma} = J_{mm}$, (*2*) $2J_{ma} = J_{mm}$, and (*3*) $J_{ma} = -J_{mm}$. The thick line is the Langmuir isotherm. For explanation, see main text.

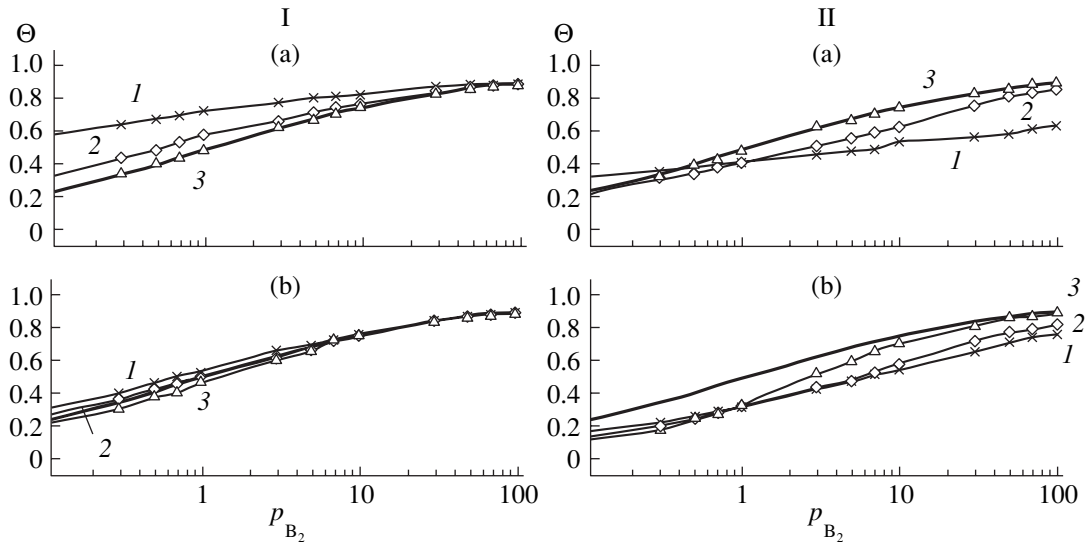

Fig. 6. Dissociative bimolecular adsorption isotherms at (Ia, IIa) 300 and (Ib, IIb) 1300 K: (*1*) $J_{ma} = J_{mm}$, (*2*) $2J_{ma} = J_{mm}$, and (*3*) $J_{ma} = -J_{mm}$. The thick line is the Langmuir isotherm. For explanation, see main text.

increases, and collective defects appear, including steps surrounding terraces (comparatively flat surface areas). The roughness of the surface increases with increasing temperature. Note that our model is limited to a temperature range that is not close to the melting point, since the BCSOS model does not allow for the formation of vacancies in the bulk.

Simulation of Adsorption and Desorption Processes

Figures 5 and 6 present monomolecular and bimolecular dissociative adsorption isotherms calculated in the framework of our model for different energies of lateral adsorbate–metal interaction (J_{ma}) and temperatures. We did not take into account the adsorbate–adsorbate interaction. The Langmuir isotherm, which is shown as a thick line, was calculated using the formula $\Theta = p/(1 + p)$ for monomolecular adsorption and the formula $\Theta = \dfrac{\sqrt{p}}{(1 + \sqrt{p})}$ for dissociative bimolecular adsorption. In the calculation of these isotherms, pressure was varied between 0.001 and 100 (in arbitrary units). For better visualization of the initial portions of the isotherms, pressure in Figs. 5 and 6 is plotted on the logarithmic scale.

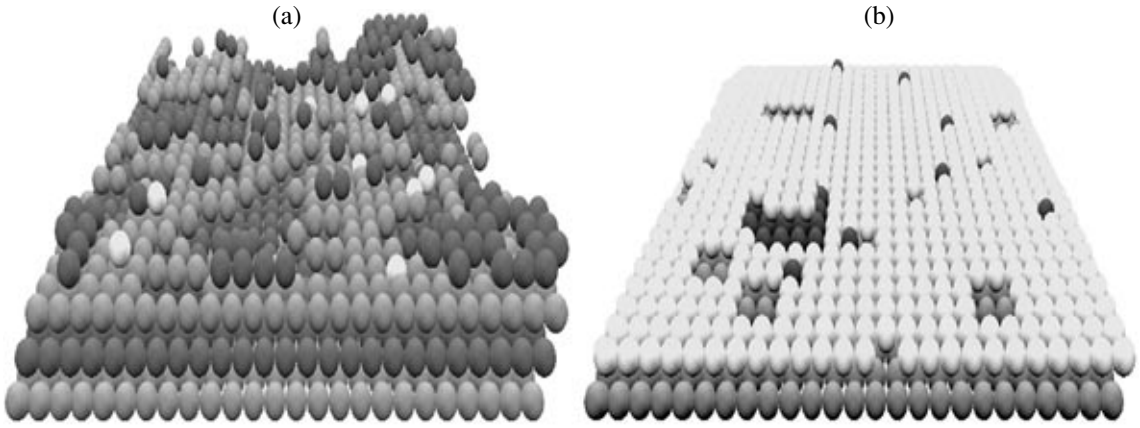

Fig. 7. Fragment of the surface at 1300 K and a (a) low and (b) high adsorbate pressure. The white spheres are adsorbate atoms.

The isotherms were calculated for two different adsorbate–metal interaction (attraction) energies: $J_{ma} = J_{mm}$ and $J_{ma} = 0.5\ J_{mm}$. For illustration, we considered the case of $J_{ma} = -J_{mm}$ (repulsion). For each pressure point, we made 200 adsorption Monte Carlo steps. One hundred of them were made to bring the system to a steady state (for the establishment of an equilibrium surface morphology and equilibrium adsorbate coverage). The subsequent 100 steps were made to average the resulting adsorbate coverage Θ (the different ways of normalizing this quantity are described below) and, accordingly, to reduce the stochastic effect of noise.

Both Fig. 5 and Fig. 6 plot Θ data normalized in two different ways: curves (I) represent surface coverages calculated as $\Theta = M/L$, and curves (II) represent the same data calculated as $\Theta = M/N \times N$, where M is the number of adsorbed species (AZ or BZ), N is the lattice size, and L is the current number of adsorption sites accessible to adsorbates. It seems impossible to interpret, in any meaningful way, the isotherms obtained using conventional normalization to the total number of adsorption sites possible on a smooth surface (Figs. 5, 6, curves II). Some portions of these isotherms lie below the Langmuir isotherm (that is, the calculated surface coverage is lower than is predicted by the Langmuir isotherm), particularly at high temperatures, and some calculated isotherms (e.g., the high-temperature monomolecular adsorption isotherm) have nonmonotonic portions, and so on. We made a special check to see if the nonmonotonic run of the isotherms and the other features described above are due to the very slow equilibration in the lattice model. However, increasing the number of Monte Carlo steps to 10000 (by two orders of magnitude) for each pressure point did not result in any appreciable change in the adsorbate coverage. The specific features of isotherms presented in the right-hand parts of Figs. 5 and 6 are due to the fact that, as the surface roughness increases, the number of unoccupied sites on the surface decreases (by a factor of ~2 at high temperatures). This decrease in the number of sites accessible to adsorbates is responsible for the fact that, if the surface coverage is normalized in a conventional way to the number of cells in the lattice, the calculated isotherms may be nonmonotonic. Therefore, the conventional normalization is inapplicable in this case and the surface coverage should be normalized to the variable number of accessible adsorption sites. Indeed, nonmonotonicity is not observed with this normalization.

The isotherms presented in the left-hand parts of Figs. 5 and 6 allow simple physical interpretation. At low temperatures, the stronger the adsorbate–metal attraction, the higher the position of the corresponding isotherm relative to the Langmuir isotherm. This is explained by the fact that the adsorbed species whose nearest neighbors are metal atoms (this is possible because the surface is rough owing to the thermal diffusion of metal atoms) are desorbed with a lower probability. The adsorbate–surface binding energy for these species is higher than the same energy in the case of a smooth surface. At high temperatures, both the monomolecular and bimolecular adsorption isotherms are close to the Langmuir isotherm, because the dimensionless adsorbate–metal interaction energies are low (here, the dimensionless energy is E/kT). Note that the isotherms in the case of adsorbate–metal repulsion are slightly below the Langmuir isotherm, since the probability of desorption in this case is higher and, furthermore, this interaction favors the smoothening of the surface.

An interesting effect is that a heavily distorted surface is smoothened as the gas pressure is gradually raised, that is, as the adsorbate coverage of the surface increases (Fig. 7). This effect is not observed for the primitive cubic lattice [25–27]. This is explained by the fact that adsorption on the bcc crystal surface requires an even area made up of four atoms for monomolecular adsorption and of six atoms for bimolecular adsorption. After adsorption, this area persists until the adsorbate leaves the occupied adsorption site.

Simulation of the Reaction

We carried out a series of numerical experiments in the framework of the above model. In each experiment, we gradually increased the mole fraction of substance A in the gas phase ($Y_A = p_A/(p_A + p_{B_2})$). For each Y_A value, we performed 50000 adsorption Monte Carlo steps (each step included N^2 adsorption–desorption trials). When the diffusion of metal and AZ atoms on the surface was taken into account, each adsorption trial was followed by 20 metal atom and AZ diffusion events for thermodynamic equilibration.

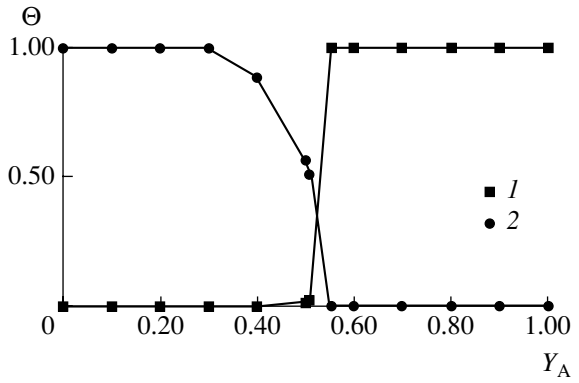

Fig. 8. Adsorbate coverage as a function of Y_A for the smooth metal surface on which no diffusion of metal or AZ atoms takes place: (*1*) AZ and (*2*) BZ.

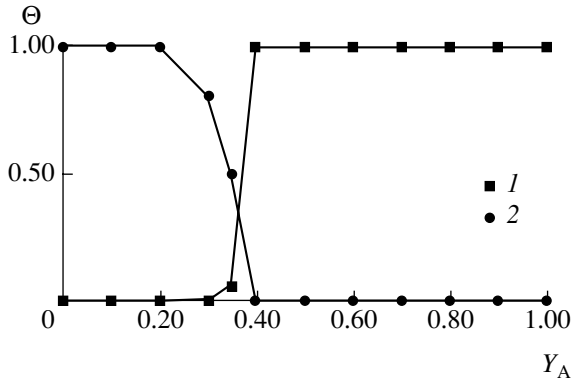

Fig. 9. Dependence of the adsorbate coverage on Y_A taking into account the diffusion of metal and AZ atoms on the surface: (*1*) AZ and (*2*) BZ.

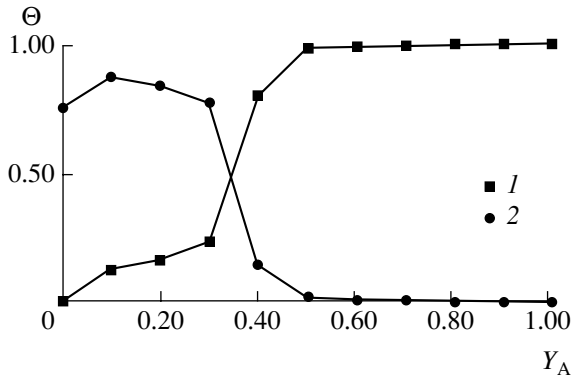

Fig. 10. Adsorbate coverage as a function of the mole fraction of A in the gas phase for a preliminarily roughened surface on which no diffusion of metal or AZ atoms takes place: (*1*) AZ and (*2*) BZ.

As for a smooth surface on which no diffusion takes place and $k_{des,A} = 0$, the calculated data are in agreement with the data following from the classical ZGB model [35]. (This is indirect evidence that our model is valid.) The dependence of the adsorbate coverage of the metal surface on the mole fraction of A in the gas phase in this case is plotted in Fig. 8. The adsorbate coverage was calculated as the ratio of the number of adsorbate atoms on the surface to the real number of adsorption sites. For a smooth surface, the latter number is $N \times N$; however, it can be reduced by the diffusion of metal atoms.

Let us discuss, in brief, the mechanism of the formation of a complete BZ coverage at small Y_A values. In the case of the random adsorption of diatomic molecules onto a smooth surface, the BZ coverage does not exceed ~0.91 (if no diffusion takes place). If AZ and BZ react, then AZ atoms will be adsorbed on separate empty sites, which are necessarily present in the BZ adsorption layer. This will be followed by the formation of a pair of empty sites through an instantaneous reaction between AZ and the nearest-neighbor BZ atom. The resulting pair of neighboring sites will be primarily occupied by BZ atoms, because $p_{B_2} \gg p_A$. Since this process requires the presence of AZ atoms on the surface, the complete BZ coverage is possible only at $Y_A \neq 0$. For this reason, in the calculation of steady-state coverages in the ZGB model, a sufficiently small, but nonzero, Y_A value ($Y_A = 0.01$) is usually taken to be the initial point.

Introducing the diffusion of surface metal atoms into the model (taking into account the roughening of the surface) shifts the points of first- and second-order kinetic phase transitions to smaller Y_A values (Fig. 9). This is explained by the fact that the roughened surface makes the adsorption of B_2 difficult (a flat site consisting of six atoms is necessary for successful adsorption).

For a reaction carried out on a preliminarily roughened surface on which no metal diffusion takes place, there is no Y_A range in which the surface is completely covered with BZ (Fig. 10) and essentially different kinetics are observed. The main factor in this case is the steric hindrance preventing B_2 adsorption. The kinetic phase transitions that occur on a smooth surface and on a rough surface with a variable morphology (Figs. 8, 9) are not observed on a "frozen" rough surface.

If the reaction is carried out on a preliminarily roughened surface and the subsequent morphological changes are taken into account (Fig. 11), there is again a range of small Y_A values in which the surface is com-

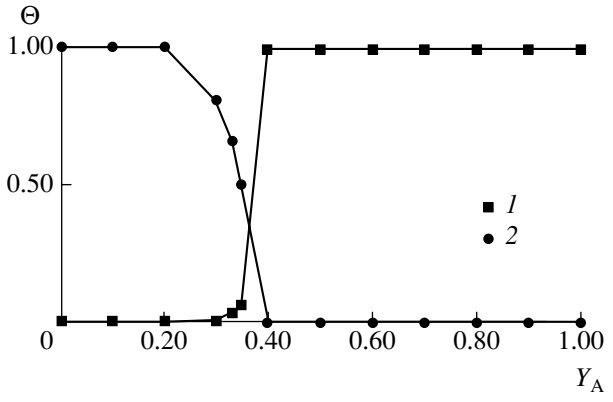

Fig. 11. Adsorbate coverage as a function of the mole fraction of A in the gas phase for a preliminarily roughened surface on which the diffusion of metal and AZ atoms is allowed: (*1*) AZ and (*2*) BZ.

pletely covered with BZ, but the second-order kinetic phase transition occurs at a smaller Y_A value than the same transition in the ZGB model (Fig. 8). This is explained by the smoothening of the surface owing to the adsorption of B_2 molecules, which dominate the gas phase. The first-kind kinetic phase transition is also shifted to smaller Y_A values (as in the case depicted in Fig. 9) because of the steric hindrance hampering B_2 adsorption.

Thus, the most important results of this study are as follows:

(1) An imitation model based on the Kossel crystal model (which is well known in physics) is constructed for adsorption and chemical reaction on the (100) face of a bcc crystal whose morphology varies under the action of external factors (temperature and surface coverage).

(2) In the model suggested here, adsorption smoothens the originally rough surface owing to the stabilization of flat areas by adsorbate molecules, as distinct from adsorption in a similar model for the primitive cubic lattice.

(3) In our model, as distinct from models with a fixed surface morphology, the number of accessible adsorption sites varies dependings on external conditions.

(4) Taking into account the thermal mobility of catalyst atoms in the simulation of reactions proceeding by the adsorption mechanism shifts the point of the first-order kinetic phase transition to lower monomolecular component partial pressures relative to the same transition in the ZGB model. This is explained by the unfavorable effect of the rough surface on bimolecular adsorption.

REFERENCES

1. Zhdanov, V.P. and Kasemo, B., *Surf. Sci. Rep.,* 2000, vol. 39, p. 25.
2. Kang, H.C. and Weinberg, W.H., *Surf. Sci.*, 1994, vols. 299/300, p. 755.
3. Van Hove, M.A. and Somorjai, G.A., *Surf. Sci.*, 1994, vols. 299/300, p. 487.
4. Norskov, J.K., *Surf. Sci.*, 1994, vols. 299/300, p. 690.
5. Libuda, J. and Freund, H.-J., *J. Phys. Chem. B*, 2002, vol. 106, p. 4901.
6. Zaera, F., *Surf. Sci.,* 2002, vol. 500, p. 947.
7. Zhdanov, V.P., *Surf. Sci.*, 2002, vol. 500, p. 966.
8. Binder, K., *J. Comput. Phys.*, 1985, vol. 59, p. 1.
9. Williams, E.D., *Surf. Sci.*, 1994, vols. 299/300, p. 502.
10. Conrad, E.H. and Engel, T., *Surf. Sci.*, 1994, vols. 299/300, p. 391.
11. Inaoka, T. and Yoshimori, A., *Surf. Sci.*, 1982, vol. 115, p. 301.
12. Myshlyavtsev, A.V. and Zhdanov, V.P., *J. Chem. Phys.*, 1990, vol. 92, p. 3909.
13. Zhdanov, V.P., *Surf. Sci.*, 1992, vol. 277, p. 155.
14. Imbihl, R., Reynolds, A.E., and Kaletta, D., *Phys. Rev. Lett.*, 1991, vol. 67, p. 275.
15. Reynolds, A.E., Kaletta, D., Ertl, G., and Behm, R.J., *Surf. Sci.*, 1989, vol. 218, p. 452.
16. Monine, M.I. and Pismen, L.M., *Catal. Today,* 2001, vol. 70, p. 311.
17. Monine, M.I. and Pismen, L.M., *Phys. Rev. E*, 2002, vol. 66, art. 051601.
18. Monine, M.I. and Pismen, L.M., *Phys. Rev. E*, 2004, vol. 69, art. 021606.
19. Van Beijeren, H., *Phys. Rev. Lett.*, 1977, vol. 38, p. 993.
20. Gilmer, G.H. and Bennema, P., *J. Appl. Phys.*, 1972, vol. 43, p. 1347.
21. Bracco, G., *Phys. Low-Dimens. Semicond. Struct.,* 1994, vol. 8, p. 1.
22. Lapujoulade, J., *Surf. Sci. Rep.*, 1994, vol. 20, p. 191.
23. Rys, F.S., *Ber. Bunsen-Ges. Phys. Chem.*, 1986, vol. 90, p. 208.
24. Kossel, W., *Nachr. Akad. Wiss. Goettingen, Math. Phys. Kl.*, 1927, p. 135.
25. Resnyanskii, E.D., Latkin, E.I., Myshlyavtsev, A.V., and Elokhin, V.I., *Chem. Phys. Lett.*, 1996, vol. 248, p. 136.
26. Resnyanskii, E.D., Myshlyavtsev, A.V., Elokhin, V.I., and Bal'zhinimaev, B.S., *Chem. Phys. Lett.*, 1997, vol. 264, p. 174.
27. Elokhin, V.I., Myshlyavtsev, A.V., Latkin, E.I., Resnyanskii, E.D., Sheinin, D.E., and Bal'zhinimaev, B.S., *Kinet. Katal.,* 1998, vol. 39, no. 2, p. 264 [*Kinet. Catal.* (Engl. Transl.), vol. 39, no. 2, p. 246].
28. Zhdanov, V.P. and Kasemo, B., *Phys. Rev. B: Condens. Matter*, 1997, vol. 56, p. 10067.
29. Zhdanov, V.P. and Kasemo, B., *J. Chem. Phys.*, 1998, vol. 108, p. 4582.
30. Zhdanov, V.P. and Kasemo, B., *Surf. Sci.*, 1998, vol. 418, p. 84.
31. Aldao, C.M., Guidoni, S.E., Xu, G.J., Nakayama, K.S., and Weaver, J.H., *Surf. Sci.*, 2004, vol. 551, p. 143.

32. Vakarin, E.V., Filippov, A.E., and Badiali, J.P., *Phys. Rev. Lett.,* 1999, vol. 81, p. 3904.

33. Vakarin, E.V., Filippov, A.E., Badiali, J.P., and Holovko, M.F., *Phys. Rev. E*, 1999, vol. 60, p. 660.

34. Metropolis, N., Rosenbluth, A.V., Rosenbluth, M.N., Teller, A.H., and Teller, E., *J. Chem. Phys.*, 1953, vol. 21, p. 1087.

35. Ziff, R.M., Gulari, E., and Barshad, Y., *Phys. Rev. Lett.*, 1986, vol. 56, p. 2553.

36. Zhdanov, V.P. and Kasemo, B., *Surf. Sci. Rep.,* 1994, vol. 20, p. 111.

37. Albano, E.V., *Heter. Chem. Rev*, 1996, vol. 3, p. 389.

38. Yablonskii, G.S., Bykov, V.I., Gorban, A.N., and Elokhin, V.I., in *Comprehensive Chemical Kinetics*, vol. 32: *Kinetic Models of Catalytic Reactions*, Compton, R.G., Ed., Amsterdam: Elsevier, 1991, ch. 6.

39. Lewis, R. and Gomer, R., *Surf. Sci.,* 1968, vol. 12, p. 157.

40. Gomer, R., *Rep. Progr. Phys.,* 1990, vol. 53, p. 917.

41. Imbihl, R., *Prog. Surf. Sci.*, 1993, vol. 44, p. 185.

42. Kislyuk, M.U., *Kinet. Katal.*, 1998, vol. 39, no. 2, p. 246 [*Kinet. Catal.* (Engl. Transl.), vol. 39, no. 2, p. 229].